

Article

Day-Ahead Two-Stage Bidding Strategy for Multi-Photovoltaic Storage Charging Stations Based on Bidding Space

Fulu Yan *, Lifeng Wei, Jun Yang and Binbin Shi

Linfen Power Supply Company, State Grid Electric Power Company, Linfen 041000, China

* Correspondence: yanfulu@sx.sgcc.com.cn

Abstract: Against the backdrop of a “dual-carbon” strategy, the use of photovoltaic storage charging stations (PSCSs), as an effective way to aggregate and manage electric vehicles, new energy sources, and energy storage, will be an important primary component of the electricity market. The operational characteristics of the aggregated resources within a PSCS determine its bidding space, which has an important influence on its bidding strategy. In this paper, a novel bidding space model is constructed for PSCSs, which dynamically integrates electric vehicles, photovoltaic generation, and energy storage. A two-stage bidding strategy for multiple PSCSs is established, with stage I aiming at achieving the lowest cost for the power purchased by a PSCS to optimize the power generation and power plan and stage II aiming at achieving the lowest cost of the grid operator’s power purchase to optimize the system’s power balance. Thirdly, the two-stage model is transformed into a single-layer, mixed-integer linear programming problem using dyadic theory and Karush–Kuhn–Tucker (KKT) conditions, enabling the derivation of the optimal bidding strategy. Finally, the example analysis verifies that the proposed model can achieve a reduction in the PSCS’s day-ahead power purchase cost and flexibly dispatch each resource within the PSCS to maximize revenue, as well as reducing power consumption behavior during peak tariff hours, to enhance the market power of the PSCS in the electricity market.



Academic Editor: Vladimir Katic

Received: 22 November 2024

Revised: 27 December 2024

Accepted: 28 December 2024

Published: 14 January 2025

Citation: Yan, F.; Wei, L.; Yang, J.; Shi, B. Day-Ahead Two-Stage Bidding Strategy for Multi-Photovoltaic Storage Charging Stations Based on Bidding Space. *World Electr. Veh. J.* **2025**, *16*, 41. <https://doi.org/10.3390/wevj16010041>

Copyright: © 2025 by the authors. Published by MDPI on behalf of the World Electric Vehicle Association. Licensee MDPI, Basel, Switzerland. This article is an open access article distributed under the terms and conditions of the Creative Commons Attribution (CC BY) license (<https://creativecommons.org/licenses/by/4.0/>).

Keywords: photovoltaic storage charging station; centralized dispatch; bidding space; two-layer bidding strategy; KKT condition

1. Introduction

With the implementation of the “dual-carbon” strategy, greater access to renewable energy and electric vehicles (EVs) has become one of the important features of the new power system [1–3]. However, new energy generation and EV loads show significant stochasticity and volatility, which bring many threats and challenges to the safe and stable operation of the power grid [4,5]. This puts greater demands on the power system in terms of flexibility regulation, load matching, and capital investment [6–8].

To minimize the threat of new energy volatility to the security and stability of power systems, in recent years, domestic and foreign countries have introduced policies related to the participation of PSCSs in the power market and encouraged the inclusion of EVs in the market [9–11]. PSCSs, as a new type of energy management and optimization tool, can integrate and dispatch distributed energy resources (e.g., electric vehicle clusters (EVCs), energy storage devices, and photovoltaic (PV) power generation systems) distributed in different locations, which is of great significance in terms of enhancing energy utilization efficiency, optimizing the operation of the electricity market, and safeguarding the stability of the power system.

According to Shanxi market trading rules, PSCSs in the power market need to report the volume offer and operate according to the clearing curve. When determining the bidding strategy of a PSCS, the source–load characteristics of the resources it aggregates must be taken into account to assess its overall bidding space and determine the volume–price curve information, such as traded power, price, and net loads, to reduce the bias in the assessment caused by the deviation between the clearing power and the actual traded power [12]. Considering multiple factors, such as energy usage habits, price, and PV uncertainty, for each participant in a PSCS in synergy with each other, accurately assessing the overall bidding space of the PSCS and formulating a reasonable bidding strategy are key to improving the revenue of the PSCS market [13–15].

Regarding the bidding space, Ref. [16] proposes a bidding strategy for charging stations with energy storage systems that utilizes the flexibility of these energy storage systems to increase economic benefits. The authors of [17] propose a bidding strategy for the mobile charging of EVs to effectively increase the revenue of charging stations and reduce charging costs for EV users. Furthermore, Ref. [18] proposes an EV bidding auction mechanism for charging stations in microgrids to facilitate the trading of energy between EVs and charging stations. The authors of [19] propose a day-ahead bidding strategy for clusters of charging stations integrated with energy storage systems to improve their revenue. The authors of Ref. [20] present a hierarchy-based, decentralized energy management strategy for PV-based charging stations. However, these studies typically do not consider competitive interactions between multiple charging stations, which is crucial when several charging station operators (CSOs) participate in the electricity market. Thus, there is a lack of systematic analysis regarding competition and cooperation among multiple charging stations. The authors of Ref. [21] propose a novel multi-session EV joint bidding and pricing strategy that takes into account interactions between distribution system operators (DSOs) and EV users. The authors of Ref. [22] propose an imbalanced liability trading cooperation platform aimed at profit generation for aggregators in a real-time market from an individual perspective. Although Refs. [21,22] explore bidding strategies for multiple CSOs, they mainly focus on interactions between distribution system operators (DSOs) and EV users or real-time market imbalances, without delving into how multiple CSOs can coordinate their bidding strategies in the day-ahead market, particularly when considering factors like energy storage and PV generation. Existing studies largely overlook the temporal correlation between energy storage, PV generation, and EVs. A comparison of the models in Refs. [16–22] is summarized in Table 1.

Table 1. A comparison with existing methods in the literature.

Literature	Research Subject	Energy Storage System	Photovoltaic
16	Single CSO	✓	×
17	Single CSO	×	×
18	Single CSO	✓	×
19	Single CSO	×	×
20	Single CSO	×	✓
21	multiple CSOs	×	×
22	multiple CSOs	×	×
This article	multiple CSOs	✓	✓

To address this gap, our paper proposes a novel bidding strategy based on a bidding space model for multiple PSCSs participating in the day-ahead electricity market. The key contributions of our work are as follows:

- We propose a novel bidding space model that effectively captures the competitive and cooperative interactions among multiple charging stations.

- Building on this model, we develop a two-stage day-ahead bidding framework for multiple PSCSs and a market optimization clearing method, which is solved using the Karush–Kuhn–Tucker (KKT) conditions and pairwise theory within the MATLAB environment utilizing the GUROBI solver.
- Our model incorporates the temporal correlation between energy storage systems and PV generation, which is an aspect not addressed in the existing literature.

In this paper, a bidding strategy based on bidding space for multi-PSCS participation in the day-ahead electricity market is proposed. Firstly, a PSCS bidding space model construction method is proposed. Based on this, a two-stage multi-PSCS day-ahead bidding model and a market optimization clearing method are proposed. Combining the KKT condition and pairwise theory, the two-stage model is solved based on the MATLAB environment through the GUROBI solver. The example compares the impact of different participation modes on the day-ahead power purchase cost, which verifies the accuracy and efficiency of the model and method proposed in this paper.

2. PSCS Bidding Space Model

PSCSs can aggregate EVCs, energy storage, and PV systems. Consequently, the bidding space of a PSCS is jointly constrained by all three components. In this paper, the bidding space is formulated as a spatial vector, where $P_{t,i,V}^{S,max}$ represents the upper limit of electric power used by EVCs, $P_{t,i,V}^{D,max}$ denotes the upper limit of discharge power, $S_{t,i,V}^{min}$ and $S_{t,i,V}^{max}$ are the lower and upper limits of the electric energy of EVCs at each moment, $\Delta S_{t,i,V}$ signifies the change in the electric energy of EVCs due to the change in grid-connected status, and $P_{t,i,P}^{D,max}$ indicates the upper limit of PV power output. Among these parameters, the output of the energy storage system must be flexibly adjusted according to the prediction results of PV and EVCs, as well as tariff information. Therefore, the PSCS bidding space $COCT_i$ is shown in Figure 1, and its mathematical expression is presented as follows:

$$COCT_i = \left(P_{t,i,V}^{S,max}, P_{t,i,V}^{D,max}, S_{t,i,V}^{min}, S_{t,i,V}^{max}, P_{t,i,P}^{D,max} \right) \quad (1)$$

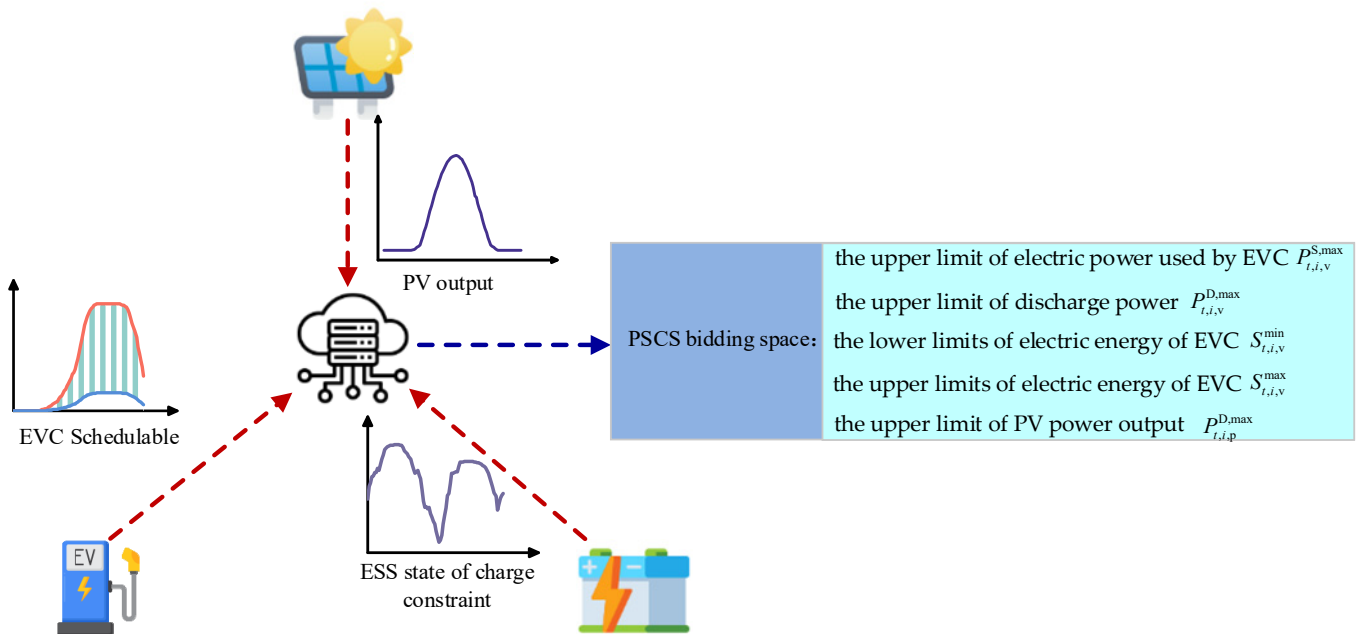


Figure 1. PSCS bidding space.

2.1. EVC Schedulable Space

Through the Vehicle-to-Grid technology, EVCs can be charged and discharged in PSCSs. A space vector $\{P_{t,i,v}^{S,\max}, P_{t,i,v}^{D,\max}, S_{t,i,v}^{\min}, S_{t,i,v}^{\max}, \Delta S_{t,i,v}\}$ is used to describe the dispatchable space generated by EVCs in the process of charging and discharging, and then the power and quantity boundaries generated by EVCs in the charging and discharging and grid-connecting stages in each period are derived through the EV grid connecting and grid exit times. The following formula can obtain the elements in time-dispatchable space:

$$\left\{ \begin{array}{l} P_{t,i,v}^{S,\max} = \sum_{n \in I_i^{\text{ev}}} p_n^{S,\max} W_{n,t} \\ P_{t,i,v}^{D,\max} = \sum_{n \in I_i^{\text{ev}}} p_n^{D,\max} W_{n,t} \\ S_{t,i,v}^{\min} = \sum_{n \in I_i^{\text{ev}}} s_n^{\min} W_{n,t} \\ S_{t,i,v}^{\max} = \sum_{n \in I_i^{\text{ev}}} s_n^{\max} W_{n,t} \\ \Delta S_{t,i,v} = \sum_{n \in I_i^{\text{ev}}} (s_n^{\text{arr}} W_{n,t} (W_{n,t} - W_{n,t-1}) \\ \quad - s_n^{\text{lea}} W_{n,t-1} (W_{n,t-1} - W_{n,t})) \end{array} \right. \quad (2)$$

where $W_{n,t}$ is the grid-connected state variable of the n -th EV in period t , $W_{n,t} = 1$ indicating that the EV is in the grid-connected state in period t ; otherwise, $W_{n,t} = 0$. s_n^{\max} and s_n^{\min} are the upper and lower limits of the rated power of the n -th EV, respectively. $p_n^{S,\max}$ and $p_n^{D,\max}$ are the upper limits of the rated charging and discharging power of the n -th EV, respectively. I_i^{ev} is the set of EVCs aggregated by the i -th operator PSCSi. s_n^{arr} and s_n^{lea} are the initial power when the n -th EV is connected to the grid and when it is off the grid, respectively.

2.2. Energy Storage Dispatchable Space

The dispatchable capacity of the energy storage system is determined by its rated capacity and is subject to the following constraints:

$$\left\{ \begin{array}{l} 0 \leq P_{t,i,e}^S \leq P_{t,i,e}^{S,\max} \\ 0 \leq P_{t,i,e}^D \leq P_{t,i,e}^{D,\max} \\ S_{t,i,e} = S_{t-1,i,e} (1 - \delta^{\text{ess}}) + P_{t,i,e}^D \eta^{\text{essch}} \Delta t - \frac{P_{t,i,e}^D \Delta t}{\eta^{\text{essdis}}} \\ S_{1,i,e} = S_{96,i,e} = 0.5 \times S_e^N \end{array} \right. \quad (3)$$

where $P_{t,i,e}^S$ and $P_{t,i,e}^D$ are the charging and discharging power of the energy storage system of the i -th operator PSCSi in period t , respectively. $P_{t,i,e}^{S,\max}$ and $P_{t,i,e}^{D,\max}$ are the rated charging and discharging power of the energy storage system, respectively. $S_{t,i,e}$ is the residual power of the energy storage system in period t . δ^{ess} is the self-depletion coefficient. η^{essch} and η^{essdis} are the charging and discharging loss coefficients, respectively. S_e^N is the rated power. To satisfy the system continuity constraints, this paper assumes that the energy storage power state is 50% at the beginning and end of the daily scheduling.

3. PSCS Day-Ahead Bidding Model

3.1. PSCS Day-Ahead Bidding Strategy Framework

According to the trading rules of the electricity market, PSCSs, as new market participants, participate in market bidding by integrating various resources, such as EVCs, PV power, energy storage, and so on, and adopt the competitive offer method. In scenarios where multiple PSCSs participate in the day-ahead market, each PSCS develops a corresponding bidding strategy based on its bidding space and the prevailing market

conditions to achieve cost minimization. The process of multiple PSCSs participating in the day-ahead power market is shown in Figure 2, which consists of two phases: PSCS bidding and market clearing.

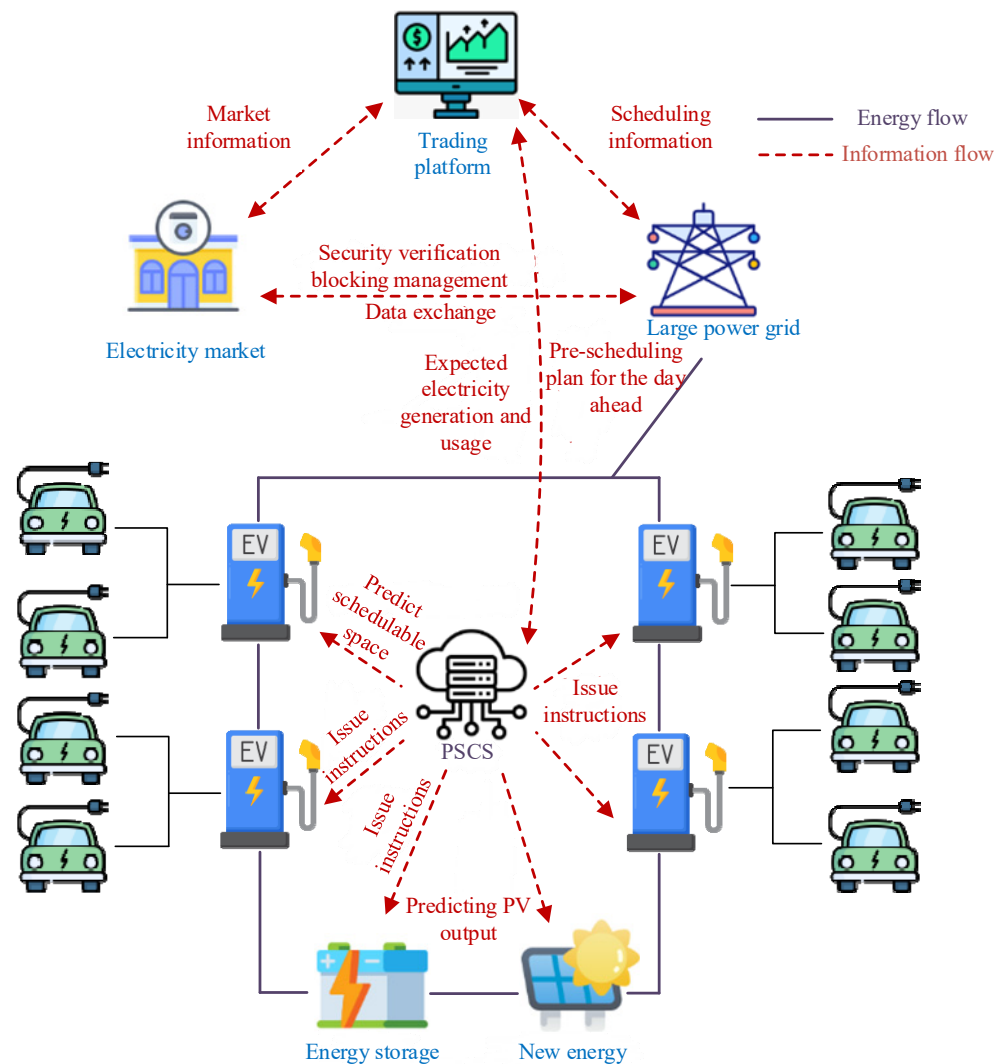


Figure 2. Day-ahead market operation process.

In the first stage, each PSCS optimizes its tariff and power mix based on its bidding space through a bidding model and submits it to the power trading center to form their respective expected generation and consumption plans. At this stage, the main objective of PSCSs is profit maximization or cost minimization. They simulate the market clearing process in the day-ahead bidding stage based on publicly available data from China's electricity market and continuously optimize their offer strategies until they are unable to reduce costs or increase profits through further adjustments, completing the solution of the bidding strategy. At this point, the interactions among PSCSs reach a Nash equilibrium, meaning that no PSCS can unilaterally adjust its strategy to achieve a better outcome.

The second stage is led by the power trading center, which conducts market clearing based on the tariff and power data submitted by each PSCS and determines and publishes the final transaction results for each PSCS. To simplify the analysis, in this paper, the offers of all generators other than PSCSs are consolidated into an equivalent generation aggregator supply curve to represent the supply side of the market. Simultaneously, the load demand of all consumers other than PSCSs is merged into a unified load demand curve. Within this framework, PSCSs adjust their strategies within their bidding space,

analogous to making strategic adjustments on a stepped supply–demand curve, and ultimately determine their respective transacted power and price through the market clearing and settlement mechanism.

3.2. PSCS Bidding Model

When PSCSs participate in the day-ahead market, each PSCS must comprehensively consider the bidding strategies of other PSCSs as well as the overall supply and demand conditions to determine its bidding scheme. To address this, this paper constructs a two-layer bidding model comprising the following steps:

In the upper model, each PSCS develops a bidding strategy aimed at minimizing its power purchase cost, thereby determining the reported tariff and power. These results are then transmitted to the lower layer.

In the lower layer, a market clearing model is designed to maximize social benefits by determining the optimal clearing power for each PSCS, which is subsequently fed back to the upper layer.

Through repeated iterations of the upper and lower layers, the iterative process ends when the price and powers reported by each PSCS satisfy the convergence conditions, at which time the optimal bidding strategy of each PSCS is finally obtained.

4. Two-Stage Multi-PSCS Market Bidding

As described in Section 3.1, the two-stage specific bidding process is described below: (1) Stage I—PSCS Bidding Model; (2) Stage II—Market Clearance Optimization Model.

4.1. Stage I—PSCS Bidding Model

The PSCS bidding model can be divided into upper and lower bidding processes as follows.

- Bidding Upper Model—PSCS Profit Maximization

The operating cost of each PSCS is the difference between the cost of purchasing electricity and the profit of selling electricity in the electricity energy market, and each PSCS determines its bidding strategy to minimize its own cost in addition to the cost of the rest of the PSCSs. So, the upper model takes the minimization of the cost of each PSCS as the objective, and the bidding strategy of the i -th PSCS is as follows:

$$\min_{\pi_{ti}, P_{ti}^S, P_{ti}^D} f_i = \sum_{t \in T} \pi_{ti} (P_{ti}^S - P_{ti}^D) \Delta t \quad (4)$$

where f_i is the day-ahead purchase cost of PSCSi, $i = 1, 2, \dots, n$. n is the total number of PSCSs. π_{ti} is the reported tariff of PSCSi in period t . P_{ti}^S is the expected power purchased by PSCSi in period t . P_{ti}^D is the expected power sold by PSCSi in period t . Δt is the time interval. T is the set of all periods on the operating day.

The PSCS demands to satisfy the internal power balance constraints:

$$P_{ti}^S - P_{ti}^D = P_{tiv}^S + P_{tie}^S - P_{tiv}^D - P_{tie}^D - P_{tip}^D \quad (5)$$

where P_{tiv}^D is the EVC discharge power of PSCSi in period t ; P_{tie}^D is the energy storage discharge power of PSCSi in period t . P_{tip}^D is the PV power of PSCSi in period t . P_{tiv}^S and P_{tie}^S are the EVC and energy storage charging power of PSCSi in period t , respectively.

To prevent the emergence of long-time peak or trough prices, it is essential for the normal operation of the distribution network and the electricity market to establish appro-

appropriate upper and lower limits of the quoted price in each period. Consequently, PSCSs are required to submit quotations within the range permitted by the power trading center:

$$\pi_{t,\min} \leq \pi_{ti} \leq \pi_{t,\max} \tag{6}$$

where $\pi_{t,\max}$ and $\pi_{t,\min}$ are the upper and lower bounds of allowable offers in the market in period t , respectively. The day-ahead offer price and the optimal EVC and storage and PV power are the decision variables of the bidding model.

- Bidding Lower Models—Market Clearance

Each PSCS simulates market clearing based on the offer strategy of each PSCS determined by the upper layer. In this paper, we consolidate all the remaining generator offers except the PSCS to one generator’s quoted quantity offer curve and return the clearing results to the upper layer to determine the cost of each PSCS under that bidding strategy and further iteratively search for the optimal one.

Market clearing takes place as a function of minimizing the grid operator’s power purchase costs, including the cost of purchasing power from equivalent generators and the cost of net purchasing power from PSCSs.

$$\min_{P_{ti}^S, P_{ti}^D, P_{m,t}^G, P_{ab,t}} \left(\sum_{t \in T} \sum_{m \in N_{step}} \pi_m^G P_{m,t}^G \Delta t + \sum_{t \in T} \sum_{i \in N_{VPP}} \pi_{ti} (P_{ti}^D - P_{ti}^S) \Delta t \right) \tag{7}$$

where π_m^G is the price of the generator’s m -th offer segment. $P_{m,t}^G$ is the power of the generator’s m -th offer segment. N_{step} is the aggregation of the generator’s offer segments. N_{VPP} is the aggregation of the PSCS participating in the bidding. π_{ti} is the day-ahead locational marginal price (LMP) cleared by the power trading center.

The PSCS develops its bidding strategy using its bidding space as a constraint on the power and capacity of the EVC, storage, and PV equipment, as shown in Equations (8)–(18), with Equations (13) and (14) as constraints on storage powering 50% of its rated capacity at the end and beginning of each day’s dispatch.

$$0 \leq P_{tiv}^S \leq P_{tiv}^{S,\max} \tag{8}$$

$$0 \leq P_{tie}^S \leq P_{tie}^{S,\max} \tag{9}$$

$$0 \leq P_{tiv}^D \leq P_{tiv}^{D,\max} \tag{10}$$

$$0 \leq P_{tie}^D \leq P_{tie}^{D,\max} \tag{11}$$

$$0 \leq P_{tip}^D \leq P_{tip}^{D,\max} \tag{12}$$

$$S_{1,ie} = 0.5 \times S_e^N \tag{13}$$

$$S_{96,ie} = 0.5 \times S_e^N \tag{14}$$

$$S_{tie} = S_{t-1,ie} (1 - \delta^{ess}) + P_{tie}^S \eta^{essch} \Delta t - \frac{P_{tie}^D \Delta t}{\eta^{essdis}} \tag{15}$$

$$S_{tiv} = S_{t-1,iv} + \Delta S_{tiv} + P_{tiv}^S \eta^{evch} \Delta t - \frac{P_{tiv}^D \Delta t}{\eta^{evdis}} \tag{16}$$

$$S_{tie}^{\min} \leq S_{tie} \leq S_{tie}^{\max} \tag{17}$$

$$S_{tiv}^{\min} \leq S_{tiv} \leq S_{tiv}^{\max} \tag{18}$$

where Δt is the current period. η^{evch} and η^{evdis} are the EV charging and discharging efficiency, respectively. S_{tie} and S_{tiv} are the remaining power of the energy storage system and EVC in PSCSi in period t .

The distribution network node power balance and line transmission capacity constraints are as follows:

$$P_{ab,t} - \sum_{c \in w_b} P_{bc,t} = P_{tb}^L + P_{tb}^S - P_{tb}^D \quad \forall a, b \in N_L \quad (19)$$

$$-P_{ab,max} \leq P_{ab,t} \leq P_{ab,max} \quad (20)$$

where $P_{ab,t}$ is the transmission power of the branch (a, b) , and (a, b) denotes the directed branch from node a to node b , i.e., node a is the superior node of node b , and node b is the subordinate node of node a . w_b is the set of child nodes of node b . P_{tb}^L is the regular load of node b in period t . N_L is the set of nodes of the distribution network. P_{tb}^S and P_{tb}^D are the power consumption power and the power generation power of the PSCS at node b , respectively. The value of the power consumption power and the power generation power of the PSCS at node b is 0 if there is no access to the PSCS at node b . The overall power generation and consumption balance constraint is as follows:

$$\sum_{m \in N_{step}} P_{m,t}^G = \sum_{b \in w_0} P_{0b,t} \quad \forall t \in T \quad (21)$$

where w_0 is the set of child nodes of the bus branch of the power plant. $P_{0b,t}$ is the power at time t of the node whose parent node is the bus branch of the power plant. The Generator Step Offer Segment Capacity Constraints are as follows:

$$0 \leq P_{m,t}^G \leq P_m^{G,max} \quad \forall m \in N_{step}, \forall t \in T \quad (22)$$

where $P_m^{G,max}$ is the capacity cap for the generator's m -th step offer segment.

- Game Equilibrium Analysis

In the two-layer bidding model of Equation (4) to Equation (22), the offer and power in the upper problem of the bidding are endogenously generated by the lower problem. This creates a coupling relationship between the upper and lower layers, ensuring that the final offer in the PSCS is the node marginal power price that takes into account the physical constraints of the system. As shown in Figure 3, the bidding decisions of each PSCS are resolved using iterative and stationing methods until no party can improve its revenue by changing its decision. This non-cooperative bidding among the PSCSs forms a Nash game. Additionally, there exists a decision sequence between the PSCSs and the power trading center, establishing a master-slave game dynamic. Consequently, the two-layer bidding problem evolves into a mathematical program with equilibrium constraints (MPEC) planning problem.

The objective function F_i of PSCSi is shown in Figure 3. x_i is the decision variable of PSCSi. y is the decision variable of the lower-level clearing problem. G_i and H_i are the constraints of PSCSi, respectively. f is the objective function of the clearing problem. g and h are the constraints of the clearing problem. λ and μ are the dyadic variables of the market clearing problem.

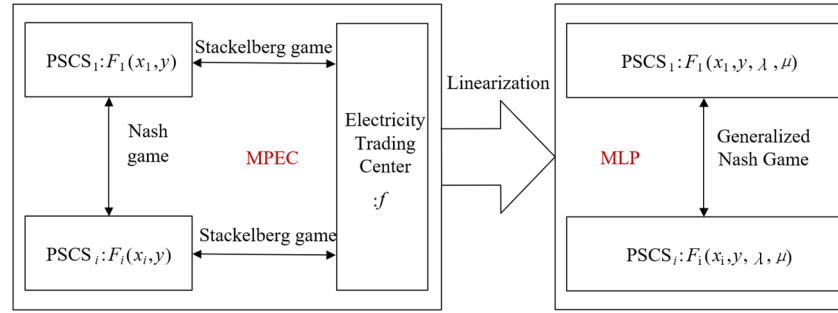


Figure 3. PSCS game relationship.

4.2. Stage II—Market Clearance Optimization Model

Each PSCS obtains its offer strategy through the first stage of the PSCS bidding model and reports the offer strategy and the desired generation plan to the power trading center. The power trading center carries out clearing optimization based on the offer strategy. Market clearing optimization is performed through the power tracking function to satisfy the desired power curves of each PSCS as much as possible.

In this paper, we set the objective function for tracking the expected power of each PSCS in the optimal clearing of the power exchange as follows:

$$\min_{P_{ii}^S, P_{ii}^D} f_{DA}^{DSO} = \sum_{t \in T} \sum_{i \in N^{VPP}} (P_{ii,cl}^S - P_{ii}^S)^2 + \sum_{t \in T} \sum_{i \in N^{VPP}} (P_{ii,cl}^D - P_{ii}^D)^2 \tag{23}$$

where $P_{ii,cl}^S$ and $P_{ii,cl}^D$ are the power purchased and sold by PSCSi in the final clearing, respectively. The market optimization clearing needs to satisfy the power ceiling constraint in the first place:

$$0 \leq P_{ii}^S \leq \sigma_{ii}^S P_{ii}^{S,max}, \forall i \in N^{VPP}, \forall t \in T \tag{24}$$

$$0 \leq P_{ii}^D \leq \sigma_{ii}^D P_{ii}^{D,max}, \forall i \in N^{VPP}, \forall t \in T \tag{25}$$

$$\sigma_{ii}^S + \sigma_{ii}^D \leq 1, \forall i \in N^{VPP}, \forall t \in T \tag{26}$$

where σ_{ii}^S and σ_{ii}^D are 0–1 variables. $\sigma_{ii}^S = 1$ and $\sigma_{ii}^D = 0$ denote that the PSCS is using electricity. $\sigma_{ii}^S = 0$ and $\sigma_{ii}^D = 1$ denote that the PSCS is generating electricity. This constraint ensures that the PSCS cannot purchase and sell electricity at the same time.

The optimal clearing of the power trading center is still based on the objective of minimizing the power purchase cost of the grid operator, as shown in Equation (7), i.e., solving the two-layer optimization problem with Equations (23)–(26) as the upper model and Equations (7)–(22) as the lower model.

By using the minimization of the power deviation shown in Equation (23) as the objective function based on the KKT condition of the market clearing problem, the two-layer model can be transformed into mixed-integer linear programming (MLP), which can be solved to produce the day-ahead pre-scheduling plan that is ultimately issued to each PSCS. As the number of PSCSs, periods, and system constraints increases, the problem can become very computationally intensive. However, we believe that the combination of heuristic methods, convergence criteria, decomposition, and parallelization techniques can make the problem solvable within a “reasonable” time frame for large instances.

The deviation between the reported power of the PSCS in the first phase and the optimized clearing power in the second phase is the power of PSCSi that is curtailed by the power trading center in period t :

$$P_{ii}^{RE} = (P_{ii,cl}^S - P_{ii}^S) - (P_{ii,cl}^D - P_{ii}^D) \tag{27}$$

4.3. The Linearization of the Model

To obtain a unique solution to the two-layer bidding problem, the Lagrangian method is used to transform the two-layer bidding problem into a single-layer mixed-integer linear programming problem. According to the strong dyadic theorem, the objective functions of the original and dyadic problems of the convex problem have the same value at the optimum. Thus, the dyadic problem of the original problem of the two-layer bidding model and the KKT condition are modeled in this section. The normalized expression of the day-ahead bidding model is as follows:

$$\begin{aligned}
 \min_{\pi_{ti}, P_{ti}^S, P_{ti}^D} f_i &= \sum_{t \in T} \pi_{ti} (P_{ti}^S - P_{ti}^D) \Delta t \\
 \text{s.t. } P_{ti}^S - P_{ti}^D &= P_{tiv}^S + P_{tie}^S - P_{tiv}^D - P_{tie}^D - P_{tip}^D \\
 \pi_{t, \min} &\leq \pi_{ti} \leq \pi_{t, \max} \\
 \{P_{ti}^S, P_{ti}^D\} &= \arg \min_{P_{ti}^S, P_{ti}^D, P_{m,t}^G, P_{ab,t}} \left(\sum_{t \in T} \sum_{m \in N_{step}} \pi_m^G P_{m,t}^G \Delta t + \sum_{t \in T} \sum_{i \in N^{VPP}} \pi_{ti} (P_{ti}^D - P_{ti}^S) \Delta t \right) \\
 \text{s.t. } -P_{ab, \max} &\leq P_{ab,t} \leq P_{ab, \max} \\
 P_{ab,t} - \sum_{c \in w_b} P_{bc,t} &= P_{tb}^L + P_{tb}^S - P_{tb}^D : \lambda_{ti}^D \\
 \sum_{m \in N_{step}} P_{m,t}^G &= \sum_{b \in w_0} P_{0b,t} : \lambda_t^G \\
 0 \leq P_{m,t}^G &\leq P_m^{G, \max} : \mu_{m,t}^{G, rt}, \mu_{m,t}^{G, lt} \\
 0 \leq P_{tiv}^S &\leq P_{tiv}^{S, \max} : \mu_{tiv}^{S, rt}, \mu_{tiv}^{S, lt} \\
 0 \leq P_{tie}^S &\leq P_{tie}^{S, \max} : \mu_{tie}^{S, rt}, \mu_{tie}^{S, lt} \\
 0 \leq P_{tiv}^D &\leq P_{tiv}^{D, \max} : \mu_{tiv}^{D, rt}, \mu_{tiv}^{D, lt} \\
 0 \leq P_{tie}^D &\leq P_{tie}^{D, \max} : \mu_{tie}^{D, rt}, \mu_{tie}^{D, lt} \\
 0 \leq P_{tip}^D &\leq P_{tip}^{D, \max} : \mu_{tip}^{D, rt}, \mu_{tip}^{D, lt} \\
 S_{1,ie} &= 0.5 * S_e^N \\
 S_{tie} &= S_{t-1,ie} (1 - \delta^{ess}) + P_{tie}^S \eta^{essch} \Delta t - \frac{P_{tie}^D \Delta t}{\eta^{essdis}} \\
 S_{tiv} &= S_{t-1,iv} + \Delta S_{tiv} + P_{tiv}^S \eta^{evch} \Delta t - \frac{P_{tiv}^D \Delta t}{\eta^{evdis}} \\
 S_{tie}^{\min} &\leq S_{tie} \leq S_{tie}^{\max} \\
 S_{tiv}^{\min} &\leq S_{tiv} \leq S_{tiv}^{\max}
 \end{aligned} \tag{28}$$

where $\left\{ \begin{matrix} \lambda_t^D, \lambda_t^G, \mu_{m,t}^{G, rt}, \mu_{m,t}^{G, lt}, \mu_{tiv}^{S, rt}, \mu_{tiv}^{S, lt}, \mu_{tie}^{S, rt}, \mu_{tie}^{S, lt}, \\ \mu_{tiv}^{D, rt}, \mu_{tiv}^{D, lt}, \mu_{tie}^{D, rt}, \mu_{tie}^{D, lt}, \mu_{tip}^{D, rt}, \mu_{tip}^{D, lt}, \mu_{ab,t}^{L, rt}, \mu_{ab,t}^{L, lt} \end{matrix} \right\}$ are dyadic variables.

The Lagrangian function of the lower market clearing objective function is as follows:

$$\begin{aligned}
 L^D &= \sum_{t \in T} \sum_{m \in N_{step}} \pi_m^G P_{m,t}^G \Delta t + \sum_{t \in T} \sum_{i \in N^{VPP}} \pi_{ti} (P_{ti}^D - P_{ti}^S) \Delta t - \lambda_{ti}^D (P_{ab,t} - \sum_{c \in w_b} P_{bc,t} - P_{tb}^L - P_{tb}^S + P_{tb}^D) \\
 &\quad - \mu_{m,t}^{G, lt} P_{m,t}^G - \mu_{m,t}^{G, rt} (P_m^{G, \max} - P_{m,t}^G) - \lambda_t^G \left(\sum_{m \in N_{step}} P_{m,t}^G - \sum_{b \in w_0} P_{0b,t} \right) - \mu_{ab,t}^{L, lt} (P_{ab, \max} + P_{ab,t}) \\
 &\quad - \mu_{ab,t}^{L, rt} (P_{ab, \max} - P_{ab,t}) - \mu_{tiv}^{S, lt} P_{tiv}^S - \mu_{tiv}^{S, rt} (P_{tiv}^{S, \max} - P_{tiv}^S) - \mu_{tie}^{S, lt} P_{tie}^S - \mu_{tie}^{S, rt} (P_{tie}^{S, \max} - P_{tie}^S) \\
 &\quad - \mu_{tiv}^{D, lt} P_{tiv}^D - \mu_{tiv}^{D, rt} (P_{tiv}^{D, \max} - P_{tiv}^D) - \mu_{tie}^{D, lt} P_{tie}^D - \mu_{tie}^{D, rt} (P_{tie}^{D, \max} - P_{tie}^D) - \mu_{tip}^{D, lt} P_{tip}^D \\
 &\quad - \mu_{tip}^{D, rt} (P_{tip}^{D, \max} - P_{tip}^D)
 \end{aligned} \tag{29}$$

The KKT condition is obtained by taking the partial derivatives of the decision variables in it through the stationing point method:

$$\begin{aligned}
 \pi_m^G \Delta t - \mu_{m,t}^{G,lt} + \mu_{m,t}^{G,rt} - \lambda_t^G &= 0 \\
 -\lambda_{ti}^D - \mu_{ab,t}^{L,lt} + \mu_{ab,t}^{L,rt} + \lambda_t^G &= 0 \\
 -\lambda_{ti}^D + \lambda_{t-1,i}^D - \mu_{ab,t}^{L,lt} + \mu_{ab,t}^{L,rt} &= 0 \\
 -\pi_{ti} \Delta t + \lambda_{ti}^D - \mu_{tiv}^{S,lt} - \mu_{tie}^{S,lt} + \mu_{tiv}^{D,rt} + \mu_{tie}^{D,rt} + \mu_{tip}^{D,rt} &= 0 \\
 \pi_{ti} \Delta t - \lambda_{ti}^D - \mu_{tiv}^{D,lt} - \mu_{tie}^{D,lt} - \mu_{tip}^{D,lt} + \mu_{tiv}^{S,rt} + \mu_{tie}^{S,rt} &= 0
 \end{aligned} \tag{30}$$

Furthermore, the complementary conditions for the inequality constraints can be written as follows:

$$\left\{ \begin{array}{ll}
 0 \leq P_{ab,max} + P_{ab,t} \perp \mu_{ab,t}^{L,lt} \geq 0 & 0 \leq p_{tie}^{S,max} - p_{tie}^S \perp \mu_{tie}^{S,rt} \geq 0 \\
 0 \leq P_{ab,max} - P_{ab,t} \perp \mu_{ab,t}^{L,rt} \geq 0 & 0 \leq p_{tiv}^D \perp \mu_{tiv}^{D,lt} \geq 0 \\
 0 \leq P_{m,t}^{G,max} \perp \mu_{m,t}^{G,lt} \geq 0 & 0 \leq p_{tie}^D \perp \mu_{tie}^{D,lt} \geq 0 \\
 0 \leq P_{m,t}^{G,max} - P_{m,t}^G \perp \mu_{m,t}^{G,rt} \geq 0 & 0 \leq p_{tip}^D \perp \mu_{tip}^{D,lt} \geq 0 \\
 0 \leq p_{tiv}^S \perp \mu_{tiv}^{S,lt} \geq 0 & 0 \leq p_{tiv}^{D,max} - p_{tiv}^D \perp \mu_{tiv}^{D,rt} \geq 0 \\
 0 \leq p_{tie}^S \perp \mu_{tie}^{S,lt} \geq 0 & 0 \leq p_{tie}^{D,max} - p_{tie}^D \perp \mu_{tie}^{D,rt} \geq 0 \\
 0 \leq p_{tiv}^{S,max} - p_{tiv}^S \perp \mu_{tiv}^{S,rt} \geq 0 & 0 \leq p_{tip}^{D,max} - p_{tip}^D \perp \mu_{tip}^{D,rt} \geq 0
 \end{array} \right. \tag{31}$$

where $A \perp B$ denotes that condition A is complementary to condition B , i.e., one and only one of the conditions A and B takes an equal sign.

Boolean variables are then introduced, and the complementary conditions are transformed into standard linear programming constraints using the big M method:

$$\left\{ \begin{array}{ll}
 0 \leq P_{ab,max} + P_{ab,t} \leq Mb_{ab,t}^{L,lt} & 0 \leq \mu_{tie}^{S,rt} \leq M(1 - b_{tie}^{S,rt}) \\
 0 \leq \mu_{ab,t}^{L,lt} \leq M(1 - b_{ab,t}^{L,lt}) & 0 \leq \mu_{tiv}^{S,rt} \leq M(1 - b_{tiv}^{S,rt}) \\
 0 \leq P_{ab,max} - P_{ab,t} \leq Mb_{ab,t}^{L,rt} & 0 \leq p_{tiv}^D \leq Mb_{tiv}^{D,lt} \\
 0 \leq \mu_{ab,t}^{L,rt} \leq M(1 - b_{ab,t}^{L,rt}) & 0 \leq p_{tie}^D \leq Mb_{tie}^{D,lt} \\
 0 \leq P_{m,t}^G \leq Mb_{m,t}^{G,lt} & 0 \leq p_{tip}^D \leq Mb_{tip}^{D,lt} \\
 0 \leq \mu_{m,t}^{G,lt} \leq M(1 - b_{m,t}^{G,lt}) & 0 \leq \mu_{tiv}^{D,lt} \leq M(1 - b_{tiv}^{D,lt}) \\
 0 \leq P_{m,t}^{G,max} - P_{m,t}^G \leq Mb_{m,t}^{G,rt} & 0 \leq \mu_{tiv}^{D,rt} \leq M(1 - b_{tiv}^{D,rt}) \\
 0 \leq \mu_{m,t}^{G,rt} \leq M(1 - b_{m,t}^{G,rt}) & 0 \leq \mu_{tip}^{D,lt} \leq M(1 - b_{tip}^{D,lt}) \\
 0 \leq p_{tiv}^S \leq Mb_{tiv}^{S,lt} & 0 \leq p_{tiv}^{D,max} - p_{tiv}^D \leq Mb_{tiv}^{D,rt} \\
 0 \leq p_{tie}^S \leq Mb_{tie}^{S,lt} & 0 \leq p_{tie}^{D,max} - p_{tie}^D \leq Mb_{tie}^{D,rt} \\
 0 \leq \mu_{tie}^{S,lt} \leq M(1 - b_{tie}^{S,lt}) & 0 \leq p_{tip}^{D,max} - p_{tip}^D \leq Mb_{tip}^{D,rt} \\
 0 \leq \mu_{tiv}^{S,lt} \leq M(1 - b_{tiv}^{S,lt}) & 0 \leq \mu_{tie}^{D,rt} \leq M(1 - b_{tie}^{D,rt}) \\
 0 \leq p_{tiv}^{S,max} - p_{tiv}^S \leq Mb_{tiv}^{S,rt} & 0 \leq \mu_{tiv}^{D,rt} \leq M(1 - b_{tiv}^{D,rt}) \\
 0 \leq p_{tie}^{S,max} - p_{tie}^S \leq Mb_{tie}^{S,rt} & 0 \leq \mu_{tip}^{D,rt} \leq M(1 - b_{tip}^{D,rt})
 \end{array} \right. \tag{32}$$

where $\left\{ \begin{array}{l} b_{ab,t}^{L,lt}, b_{ab,t}^{L,rt}, b_{m,t}^{G,lt}, b_{m,t}^{G,rt}, b_{tiv}^{S,lt}, b_{tie}^{S,lt}, b_{tiv}^{S,rt}, \\ b_{tie}^{S,rt}, b_{tiv}^{D,lt}, b_{tie}^{D,lt}, b_{tip}^{D,lt}, b_{tiv}^{D,rt}, b_{tie}^{D,rt}, b_{tip}^{D,rt} \end{array} \right\}$ is a Boolean variable. The value of M cannot be too large or too small and needs to be determined according to the value domain of the variable being scaled.

So far, the KKT condition for the day-ahead market clearing problem can be expressed as follows:

$$C_{KKT} = \left\{ \begin{array}{l} P_{ab,t}, P_{m,t}^G, p_{tiv}^S, p_{tie}^D, \lambda_{ti}^D, \\ \lambda_t^G, \mu_{m,t}^{G,rt}, \mu_{m,t}^{G,lt}, \mu_{tiv}^{S,rt}, \mu_{tie}^{S,lt} \\ \mu_{tie}^{S,rt}, \mu_{tiv}^{S,lt}, \mu_{tiv}^{D,rt}, \mu_{tie}^{D,lt}, \\ \mu_{tie}^{D,lt}, \mu_{tip}^{D,rt}, \mu_{tip}^{D,lt}, \mu_{ab,t}^{L,rt}, \mu_{ab,t}^{L,lt} \end{array} \middle| \begin{array}{l} (19), (21) \\ (30), (32) \end{array} \right\} \tag{33}$$

where C^{KKT} is the KKT condition for the lower clearing objective function.

According to the strong dyadic theory, the original problem and the dyadic problem have the same solution at the optimal point. The equivalent expression of the objective function of the upper level of the original problem is obtained after the dyadic transformation, which in turn leads to the equivalent MLP of the day-ahead bidding problem.

$$\begin{aligned}
 & \min_{\substack{\pi_{ti}^D, S_{tie}, S_{tiv}, P_{tiv}^S, P_{tie}^S, P_{tiv}^D, \\ P_{tie}^D, P_{tip}^D, P_{tjv}^S, P_{tje}^S, P_{tje}^D, P_{tjp}^D, \\ P_{ab,t}^{L,rt}, P_{ab,max} + \sum_{t \in T} \sum_{m \in N_{step}} \mu_{m,t}^{G,rt} P_m^{G,max} \\ - \sum_{t \in T} \sum_{j \in N_{VPP}/i} \pi_{tj}^D (P_{tjv}^S + P_{tje}^S - P_{tje}^D - P_{tje}^D - P_{tjp}^D) \Delta t \\ + \sum_{t \in T} \sum_{j \in N_{VPP}/i} \mu_{tjv}^{S,rt} P_{tjv}^{S,max} + \sum_{t \in T} \sum_{j \in N_{VPP}/i} \mu_{tje}^{S,rt} P_{tje}^{S,max} \\ + \sum_{t \in T} \sum_{j \in N_{VPP}/i} \mu_{tjv}^{D,rt} P_{tjv}^{D,max} + \sum_{t \in T} \sum_{j \in N_{VPP}/i} \mu_{tje}^{D,rt} P_{tje}^{D,max} + \sum_{t \in T} \sum_{j \in N_{VPP}/i} \mu_{tjp}^{D,rt} P_{tjp}^{D,max} \\ s.t. \quad \pi_{t,min} \leq \pi_{ti} \leq \pi_{t,max} \\ S_{1,ie} = 0.5 \times S_e^N \\ S_{tie} = S_{t-1,ie} (1 - \delta^{ess}) + P_{tie}^S \eta^{esssch} \Delta t - \frac{P_{tie}^D \Delta t}{\eta^{essdis}} \\ S_{tiv} = S_{t-1,iv} + \Delta S_{tiv} + P_{tiv}^S \eta^{evch} \Delta t - \frac{P_{tiv}^D \Delta t}{\eta^{evdis}} \\ S_{tie}^{min} \leq S_{tie} \leq S_{tie}^{max} \\ S_{tiv}^{min} \leq S_{tiv} \leq S_{tiv}^{max} \\ \left\{ \begin{array}{l} P_{ab,t}, P_{m,t}^G, P_{ti}^S, P_{ti}^D, \lambda_{ti}^D \\ \lambda_t^G, \mu_{m,t}^{G,rt}, \mu_{m,t}^{G,lt}, \mu_{tiv}^{S,rt}, \mu_{tiv}^{S,lt}, \\ \mu_{tie}^{S,rt}, \mu_{tie}^{S,lt}, \mu_{tiv}^{D,rt}, \mu_{tiv}^{D,lt}, \mu_{tie}^{D,rt}, \\ \mu_{tie}^{D,lt}, \mu_{tip}^{D,rt}, \mu_{tip}^{D,lt}, \mu_{ab,t}^{L,rt}, \mu_{ab,t}^{L,lt} \end{array} \right. \quad \left. \begin{array}{l} (19), (21) \\ (30), (32) \end{array} \right\}
 \end{aligned}
 \tag{34}$$

5. Case Study

5.1. Test System and Case Design

In this section, the improved RBTS-38 node distribution system [23] is employed as an example. Four PSCSs with varying internal resource shares are established at nodes 1, 4, 5, and 7, as depicted in Figure 4. The various types of EVC, PV, and energy storage shares aggregated by each PSCS are shown in Table 2. The two-layer model is implemented and solved using the GUROBI solver within the MATLAB environment.

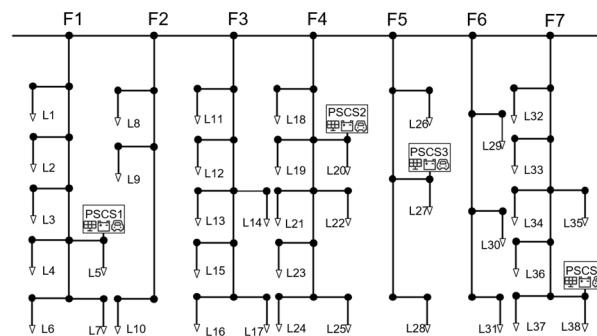


Figure 4. Improved RBTS distribution system.

Table 2. Distribution of PSCS resources.

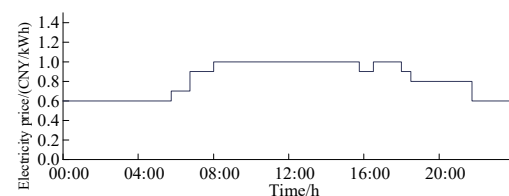
	PSCS1	PSCS2	PSCS3	PSCS4
EVC capacity/kW	1150	950	950	950
Photovoltaic capacity/kW	160	790	790	160
Energy storage capacity/(kW/kW·h)	120/240	270/540	270/540	120/240

The reasonable forecasting of conventional loads provides key information for grid operators to formulate day-ahead scheduling programs and power generation and consumption plans. There have been extensive studies on load forecasting, so this paper will not explore load forecasting techniques in depth. Based on the load curve of a typical day proposed in the literature [23], the loads of 96 periods of each feeder in the distribution system of the RBTS are set up, as shown in Table 3. While the proposed strategy is initially tailored for the day-ahead period, it can be extended to one week with the use of improved forecasting techniques, a rolling horizon approach, and scenario-based optimization.

Table 3. Time-sharing load conditions.

Time Interval	Feeder Full Load Factor							
1–8	0.61	0.61	0.61	0.61	0.58	0.58	0.58	0.58
9–16	0.57	0.57	0.57	0.57	0.57	0.57	0.57	0.57
17–24	0.59	0.59	0.59	0.59	0.64	0.64	0.64	0.64
25–32	0.76	0.76	0.76	0.76	0.88	0.88	0.88	0.88
33–40	0.96	0.96	0.96	0.96	0.98	0.98	0.98	0.98
41–48	1.00	1.00	1.00	1.00	1.00	1.00	1.00	1.00
49–56	0.97	0.97	0.97	0.97	0.97	0.97	0.97	0.97
57–64	0.93	0.93	0.93	0.93	0.89	0.89	0.89	0.89
65–72	0.90	0.90	0.90	0.90	0.94	0.94	0.94	0.94
73–80	0.91	0.91	0.91	0.91	0.86	0.86	0.86	0.86
81–88	0.84	0.84	0.84	0.84	0.83	0.83	0.83	0.83
89–96	0.76	0.76	0.76	0.76	0.67	0.67	0.67	0.67

PSCSs' power purchase prices under various decision models are shown in Figures 5 and 6. In actual electricity markets, high-tariff periods are generally not fixed for each day of the year. The timing of peak periods can vary due to several factors, including seasonal demand, weather conditions, weekdays versus weekends, and overall grid supply and demand dynamics. Thus, high-tariff periods are designed to reflect real-time demand fluctuations and are dynamically adjusted based on changing conditions in the electricity market.

**Figure 5.** Centralized dispatch mode electricity price.

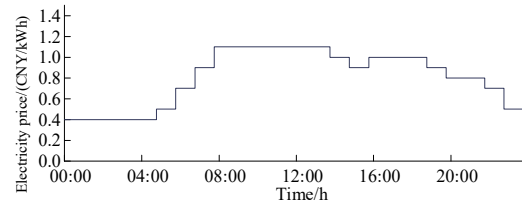


Figure 6. Price acceptance mode electricity price.

5.2. An Analysis of the Day-Ahead Charging Decision Plan

The charging decision plan of each PSCS is shown in Figures 7–10, along with the fully competitive mode, i.e., the PSCS participates in the market with the role of a price taker, and the price-setting mode, i.e., the PSCS participates in the market with the quantity–price offer mode proposed in this paper. As illustrated in the figures, under the price acceptance mode, each PSCS completes the charging of the EVC during 0:00–6:00, generally refrains from making power purchases during the high-tariff period of 8:00–12:00, and resumes power purchases during the high-tariff period of 14:00–16:00. This behavior indicates that the PSCS in the price acceptance mode can respond to price fluctuations, thereby avoiding high-cost electricity purchases during peak price periods. The flexibility of its scheduling decisions comes from the PSCS’s ability to adjust according to market prices and charging demands, thereby minimizing costs to the greatest extent. In contrast, the centralized dispatch mode results in a more delayed electricity purchase decision. Since the centralized dispatch mode is based on the minimum electricity purchase cost proposed by the ISO (Independent System Operator), its scheduling strategy focuses more on long-term cost optimization at the system level and cannot quickly respond to market price fluctuations. Consequently, the PSCS’s scheduling plans are typically preset and cannot be adjusted promptly to cope with short-term price volatility, resulting in potentially higher purchase costs, especially when prices rise rapidly.

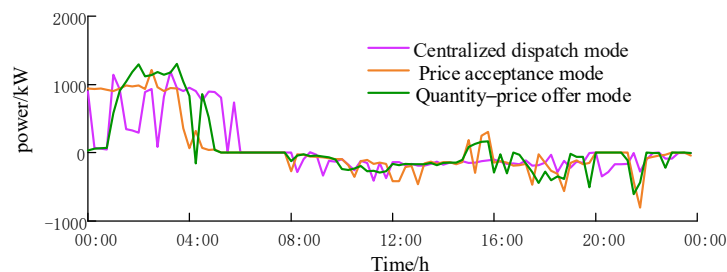


Figure 7. Comparison of pre-dispatch schedule for PSCS1.

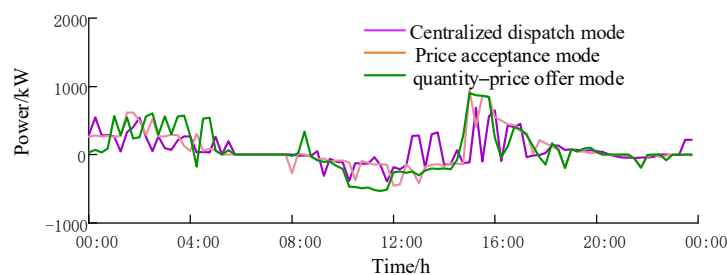


Figure 8. Comparison of pre-dispatch schedule for PSCS2.

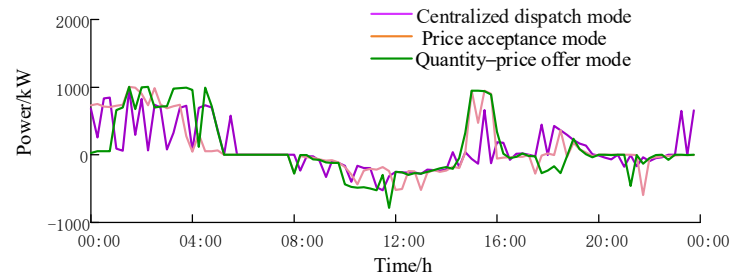


Figure 9. Comparison of pre-dispatch schedule for PSCS3.

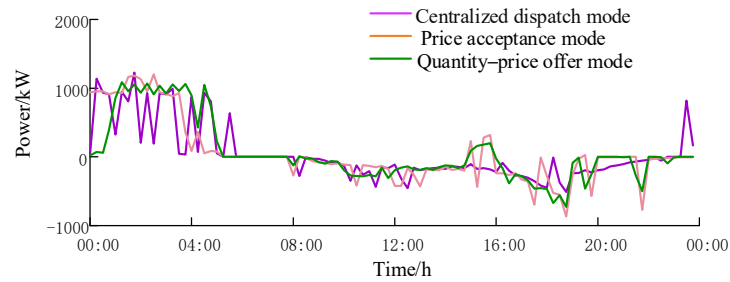


Figure 10. Comparison of pre-dispatch schedule for PSCS4.

5.3. Analysis of Cost of Day-Ahead Electricity Purchased

Table 4 illustrates that the power purchase costs in the price acceptance mode are significantly lower than those in the centralized dispatch mode. However, the power purchase costs of PSCS3 and PSCS4 in the quantity-price offer mode exceed those of the price acceptance mode. This increase is attributed to the quantity-price offers of PSCSs, which consider the bidding strategies of competitors, leading to more conservative decision-making. As a result, during high-tariff periods, such as 14:00–16:00, PSCSs are compelled to purchase electricity to meet their EVC charging demands. This conservative approach may result in higher electricity purchase costs during peak price periods. Nevertheless, this conservative strategy helps mitigate the risks arising from intense market competition, ensuring that the PSCS maintains stable operations in an uncertain market environment.

Table 4. PSCS day-ahead power purchase cost comparison.

		Participation Mode	PSCS1	PSCS2	PSCS3	PSCS4
power purchase cost		centralized dispatch mode	1638	2174	2039	1283
		price acceptance mode	1562	2088	1709	1143
		quantity-price offer mode	1473	2006	1908	1105

Table 3 shows the day-ahead power purchase costs of different PSCSs under three modes: centralized dispatch mode, price acceptance mode, and quantity-price offer mode. By comparing and analyzing the power purchase costs under different power trading modes, PSCS1 has the highest power purchase cost under the centralized dispatch mode, which is attributed to the stringent requirements for system uniformity and stability in this mode. In contrast, the cost of purchasing electricity is significantly lower in the price acceptance mode and quantity-price offer mode, especially in the quantity-price offer mode, where the cost of PSCS1 is as low as CNY 1473, indicating that it can flexibly adjust its purchasing strategy through the bidding model and effectively cope with market fluctuations, while the purchasing cost of PSCS2 is on the high end in all modes and as high as CNY 2174 in the centralized scheduling mode. This may be related to its EV cluster charging hours and higher PV (790kW) and storage (270/540kW) capacity, reflecting the challenge of optimizing PSCS2's purchasing strategy and the need for finer management

and optimization measures. PSCS3's purchasing cost in the centralized dispatch mode is CNY 2039, which is slightly lower than PSCS2's. The cost drops to CNY 1709 in the price acceptance mode but rises to CNY 1709 in the quantity–price offer mode, which is more than the price accepted by PSCS2. However, it increases to CNY 1908 in the quantity–price offer mode, indicating that PSCS3 may not be able to take full advantage of market price fluctuations for optimization in this mode and needs to adjust its bidding strategy. PSCS4 has the lowest purchase cost in all modes, even reaching as low as CNY 1105 in the quantity–price offer mode. Its lower PV (160kW) and storage (120/240kW) capacity may make it easier to manage the optimization of the power purchase strategy, allowing it to flexibly adjust its power purchase plan to maximize economic efficiency.

Among the various power trading models, PSCS1 and PSCS4 exhibit lower power purchase costs under the quantity–price offer mode, indicating that both can adjust their offers and power outputs more efficiently in this mode, thereby better adapting to market conditions. Conversely, PSCS2 and PSCS3 incur relatively lower costs under the price acceptance model, which may be attributed to their greater flexibility in responding to market price fluctuations. However, it is worth noting that the quoted offer model may lead to higher costs for PSCS3 and PSCS4, especially during high-tariff periods, when both may have to make power purchases due to the need to meet the charging demand of their EVC, thus increasing their costs.

5.4. Analysis of Quoted Prices and Quotations

This section analyzes PSCS volume–price curves for PSCSs participating in the electricity market in the quantity–price offer mode.

The bidding strategies of PSCS1 to PSCS4 are shown in Figure 11a–d. Each PSCS aims to purchase electricity during low-LMP periods to meet the charging demands of EVCs and energy storage and engage in arbitrage by selling electricity during high-price periods using EVCs and energy storage. Specifically, PSCS1–4 charge their EVCs and energy storage between 00:45 and 05:00 during low-LMP periods to charge at the lowest possible price and lay the foundation for subsequent power feedback and energy storage. At 04:15, as the LMP begins to rise, PSCSs promptly discharge energy storage to capitalize on the price increase and generate profits. Since EVCs must ensure the minimum charge required by the owner, no reverse charging is conducted during this period, and the charging state is maintained to meet the vehicle owner's requirements.

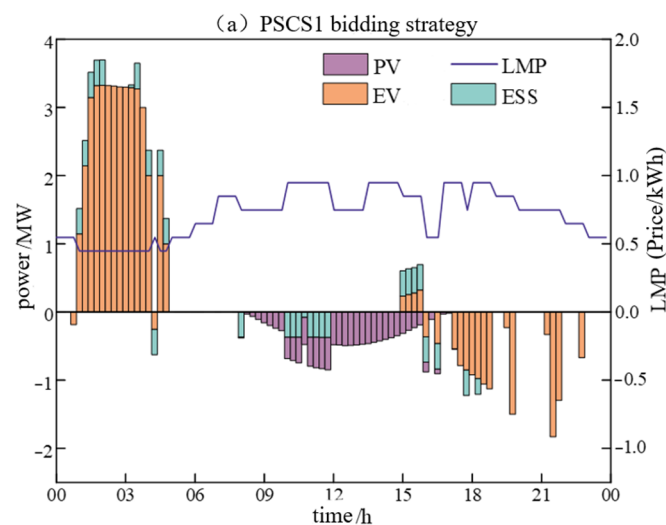


Figure 11. Cont.

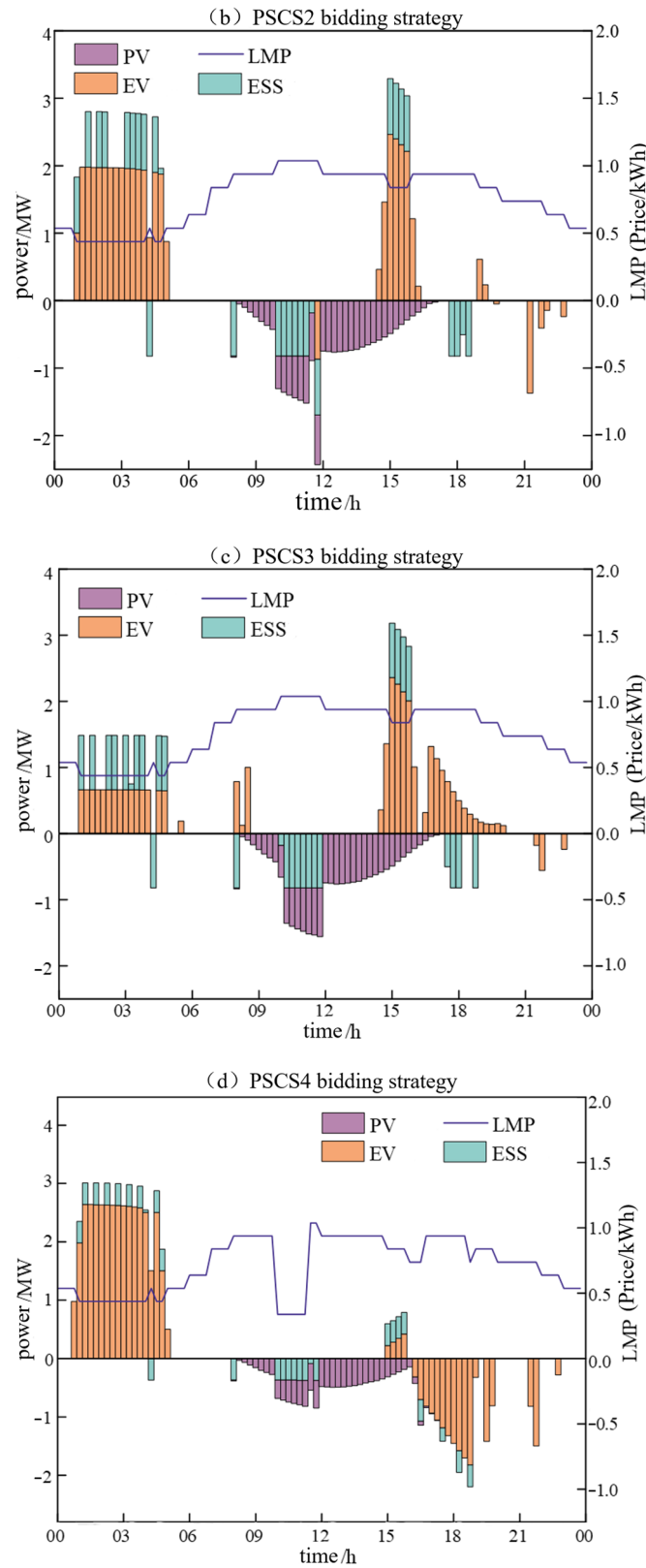


Figure 11. PSCS day-ahead bidding strategy.

Each PSCS adjusts its scheduling strategy based on the grid connection time of the EVCs. Specifically, PSCS1 discharges power to the grid between 16:00 and 22:45, PSCS2 discharges between 21:15 and 22:45, PSCS3 discharges between 21:30 and 22:45, and PSCS4 discharges between 16:15 and 22:45. PSCS1, PSCS3, and PSCS4 discharge energy from the

EVCs to the grid during these periods, utilizing the high-price periods for arbitrage. In contrast, PSCS2 has a relatively shorter feedback period and limited dispatch flexibility, potentially requiring support from energy storage or other means to take advantage of the arbitrage opportunity.

Additionally, each PSCS charges its EVCs and energy storage during photovoltaic output periods (e.g., 16:00–17:15), thereby reducing dependence on market electricity and maximizing the utilization of photovoltaic power. This scheduling strategy not only improves energy utilization efficiency but also reduces the demand for electricity purchases during high-price periods, further lowering system costs.

Through these dispatch strategies, PSCSs demonstrate a more flexible response to fluctuating electricity prices. They acquire electricity at lower costs during low-price periods and engage in arbitrage during high-price periods, thereby maximizing the system's economic benefits. Moreover, these strategies enable PSCSs to better balance electricity supply and demand amid market fluctuations, enhancing grid stability and energy efficiency. Our model incorporates not only traditional load and price forecasts but also the dispatchable space of photovoltaic generation, storage, and charging stations. We believe that this additional consideration can significantly improve the revenue of such stations. As forecasting technologies continue to improve, we expect the accuracy of predictions to increase, which will further enhance the effectiveness of the proposed strategy. When configurations change or new variables are introduced (such as variations in the resource mix, demand patterns, or market regulations), the bidding strategy model can be adapted and recalibrated to account for these changes.

6. Conclusions

In this paper, we propose a day-ahead two-stage bidding strategy for multi-PSCSs based on the bidding space. By participating in the electricity market using the quoted offer mode, the proposed PSCS can reduce its day-ahead power purchase costs and flexibly dispatch each of its resources to maximize revenue while minimizing electricity consumption during peak price hours. This approach enhances the PSCS's market power; promotes complementary interactions between the EVC, storage, and PV power; and fully leverages distributed energy sources and flexible resources with energy interaction capabilities. Furthermore, the PSCS can adjust its power and price according to day-ahead market conditions and forecasts. This flexibility allows the PSCS to respond more effectively to fluctuations in market demand, especially in the face of peak demand or shortages in power supply. In addition, the PSCS's quoted offer strategy allows it to adjust its offer in response to the behavior of other market participants, thereby remaining competitive in a highly competitive market environment.

In future work, we will explore blockchain and continuous authentication mechanisms to protect against unauthorized access and ensure the reliability of system operations. Furthermore, we will also examine the impact of existing and forthcoming government regulations on the implementation of multi-PSCS bidding strategies.

Author Contributions: F.Y.: Conceptualization, Software, and Writing—review and editing. L.W.: Visualization, Methodology, Investigation, Supervision, Original draft, and Writing—review and editing. J.Y.: Validation—review and editing. B.S.: Post-processing and Supervision—review and editing. All authors have read and agreed to the published version of the manuscript.

Funding: This research was funded by the State Grid Shanxi Electric Power Company Science and Technology Project (5205L0230005).

Data Availability Statement: The original contributions presented in this study are included in the article. Further inquiries can be directed to the corresponding author.

Conflicts of Interest: The authors declare that this study received funding from the State Grid Shanxi Electric Power Company Science and Technology Project (5205L0230005). The funder was not involved in the study design, collection, analysis, interpretation of data, the writing of this article or the decision to submit it for publication.

Nomenclature

$P_{t,i,v}^{S,max}$	the upper limit of electric power
$P_{t,i,v}^{D,max}$	the upper limit of discharge power
$S_{t,i,v}^{min}/S_{t,i,v}^{max}$	the lower/upper limits of the electric energy of the EVC
$\Delta S_{t,i,v}$	the change in the electric energy of the EVC
$P_{t,i,p}^{D,max}$	the upper limit of PV power output
$W_{n,t}$	the grid-connected state variable of the n -th EV
s_n^{max}/s_n^{min}	the upper/lower limits of the rated power of the n -th EV
$p_n^{S,max}/p_n^{D,max}$	the upper limits of the rated charging/discharging power of the n -th EV
I_i^{EV}	the set of EVCs aggregated by the i -th operator PSCSi
s_n^{arr}/s_n^{lea}	the initial power when the n -th EV is connected to the grid/when it is off the grid
$P_{t,i,e}^S/P_{t,i,e}^D$	the charging/discharging power of the energy storage system of the i -th operator PSCSi
$P_{t,i,e}^{S,max}/P_{t,i,e}^{D,max}$	the rated charging and discharging power of the energy storage system
$S_{t,i,e}$	the residual power of the energy storage system
δ^{ess}	the self-depletion coefficient
$\eta^{essch}/\eta^{essdis}$	the charging and discharging loss coefficients
S_e^N	the rated power
f_i	the day-ahead purchase cost of PSCSi
π_{ti}	the reported tariffs of PSCSi
P_{ti}^S/P_{ti}^D	the expected power purchased/sold by PSCSi
P_{tiv}^D	the EVC discharge power of PSCSi
P_{tie}^D	the energy storage discharge power of PSCSi
P_{tip}^D	the PV power of PSCSi
P_{tiv}^S/P_{tie}^S	the EVC and energy storage charging power of PSCSi
$\pi_{t,max}/\pi_{t,min}$	the upper and lower bounds of allowable offers
π_m^G	the price of the generator's m -th offer segment
$P_{m,t}^G$	the power of the generator's m -th offer segment
π_{ti}	the day-ahead locational marginal price
S_{tie}/S_{tiv}	the remaining power of the energy storage system/EVC in PSCSi
$P_{ab,t}$	the transmission power of the branch (a, b)
P_{tb}^S/P_{tb}^D	the power consumption power and the power generation power of the PSCS at node b
$P_{0b,t}$	the power at time t of the node whose parent node is the bus branch of the power plant
$P_{ti,cl}^S/P_{ti,cl}^D$	the power purchased/sold by PSCSi in the final clearing

Abbreviations

PSCS	photovoltaic storage charging station
KKT	Karush–Kuhn–Tucker
EVC	electric vehicle cluster
PV	photovoltaic
CSO	charging station operator
DSO	distribution system operator
EV	electric vehicle
MPEC	mathematical program with equilibrium constraints
MLP	mixed-integer linear programming
LMP	locational marginal price

References

1. Yang, C.; Zhao, Y.; Li, X.; Zhou, X. Electric vehicles, load response, and renewable energy synergy: A new stochastic model for innovation strategies in green energy systems. *Renew. Energy* **2024**, *238*, 121890. [[CrossRef](#)]
2. Bukhari, A.; Aboulola, O.I.; Rehman, A.U.; Alharbi, A.; Alosaimi, W.; Daud, A. Renewable energy driven on-road wireless charging infrastructure for electric vehicles in smart cities: A prototype design and analysis. *Energy Rep.* **2024**, *12*, 5145. [[CrossRef](#)]
3. Colak, A.; Fescioglu-Unver, N. Deep reinforcement learning based resource allocation for electric vehicle charging stations with priority service. *Energy* **2024**, *313*, 133637. [[CrossRef](#)]
4. Liang, Z.; Qian, T.; Korkali, M.; Glatt, R.; Hu, Q. A Vehicle-to-Grid planning framework incorporating electric vehicle user equilibrium and distribution network flexibility enhancement. *Appl. Energy* **2024**, *376*, 124231. [[CrossRef](#)]
5. Khan, M.O.; Kirmani, S.; Rihan, M. Impact assessment of electric vehicle charging on distribution networks. *Renew. Energy Focus* **2024**, *50*, 100599. [[CrossRef](#)]
6. Chen, X.; Geng, X.; Xie, D.; Gou, Z. Photovoltaic-energy storage-integrated charging station retrofitting: A study in Wuhan city. *Transp. Res. Part D Transp. Environ.* **2024**, *132*, 104241. [[CrossRef](#)]
7. Chen, X.; Gou, Z.; Gui, X. A holistic assessment of the photovoltaic-energy storage-integrated charging station in residential areas: A case study in Wuhan. *J. Build. Eng.* **2023**, *79*, 107947. [[CrossRef](#)]
8. Huang, W.; Wang, J.; Wang, J.; Zhou, M.; Cao, J.; Cai, L. Capacity optimization of PV and battery storage for EVCS with multi-venues charging behavior difference towards economic targets. *Energy* **2024**, *313*, 133833. [[CrossRef](#)]
9. Song, Y.; Liu, T.; Ye, B.; Li, Y. Linking carbon market and electricity market for promoting the grid parity of photovoltaic electricity in China. *Energy* **2020**, *221*, 118924. [[CrossRef](#)]
10. Vellachami, S.; Hasanov, A.S.; Brooks, R. Risk transmission from the energy markets to the carbon market: Evidence from the recursive window approach. *Int. Rev. Financ. Anal.* **2023**, *89*, 102715. [[CrossRef](#)]
11. Lu, Y. Idiosyncratic information spillover and connectedness network between the electricity and carbon markets in Europe. *J. Commod. Mark.* **2022**, *25*, 100185.
12. He, J.; Qi, Z. Decision-making research on multi-day rolling transaction of wind power plant under Shanxi power market system. In Proceedings of the International Conference on Computer, Artificial Intelligence, and Control Engineering (CAICE 2023), Shanghai, China, 24–26 March 2023; Shanxi Longyuan New Energy Co., Ltd. (China): Yangquan, China, 2023.
13. Domínguez-Navarro, J.A.; Dufo-López, R.; Yusta-Loyo, J.M.; Artal-Sevil, J.S.; Bernal-Agustín, J.L. Design of an electric vehicle fast-charging station with integration of renewable energy and storage systems. *Int. J. Electr. Power Energy Syst.* **2019**, *105*, 46. [[CrossRef](#)]
14. Chaudhari, K.; Ukil, A.; Kumar, K.N.; Manandhar, U.; Kollimalla, S.K. Hybrid Optimization for Economic Deployment of ESS in PV-Integrated EV Charging Stations. *IEEE Trans. Ind. Inform.* **2018**, *14*, 106. [[CrossRef](#)]
15. Raut, K.; Shendge, A.; Chaudhari, J.; Lamba, R.; Alshammari, N.F. Modeling and simulation of photovoltaic powered battery-supercapacitor hybrid energy storage system for electric vehicles. *J. Energy Storage.* **2024**, *82*, 110324. [[CrossRef](#)]
16. Duan, X.; Hu, Z.; Song, Y. Bidding Strategies in Energy and Reserve Markets for an Aggregator of Multiple EV Fast Charging Stations with Battery Storage. *IEEE Trans. Intell. Transp. Syst.* **2021**, *22*, 471. [[CrossRef](#)]
17. Liu, L.; Zhang, Z.; Xu, J.; Wang, P. A Bayesian Game Based Bidding Scheme for Mobile Charging Services in IoEV. *IEEE Trans. Serv. Comput.* **2024**, *17*, 349. [[CrossRef](#)]
18. Sarker, M.R.; Pandžić, H.; Sun, K.; Ortega-Vazquez, M.A. Optimal operation of aggregated electric vehicle charging stations coupled with energy storage. *IET Gener. Transm. Distrib.* **2018**, *12*, 1127. [[CrossRef](#)]
19. Zhao, Y.; Jia, X.; Yang, Q.; Li, D.; An, D. Towards incentive compatible auction mechanism for electric vehicles bidding in microgrids. In Proceedings of the 2018 33rd Youth Academic Annual Conference of Chinese Association of Automation (YAC), Nanjing, China, 18–20 May 2018; pp. 334–339.
20. Zhang, J.; Zhang, Y.; Li, T.; Jiang, L.; Li, K.; Yin, H.; Ma, C. A Hierarchical Distributed Energy Management for Multiple PV-Based EV Charging Stations. In Proceedings of the IECON 2018—44th Annual Conference of the IEEE Industrial Electronics Society, Washington, DC, USA, 21–23 October 2018; pp. 1603–1608.
21. Huang, C.; Wang, C.; Li, K.; Xie, N. Joint optimization of bidding and pricing strategy for electric vehicle aggregator considering multi-agent interactions. *Appl. Energy* **2024**, *360*, 122810.
22. Wu, W.; Zhu, J.; Liu, Y.; Luo, T.; Chen, Z.; Dong, H. A Coordinated Model for Multiple Electric Vehicle Aggregators to Grid Considering Imbalanced Liability Trading. *IEEE Trans. Smart Grid* **2024**, *15*, 1876–1890. [[CrossRef](#)]
23. Chowdhury, N.; Billinton, R. A reliability test system for educational purposes-spinning reserve studies in isolated and interconnected systems. *IEEE Trans. Power Syst.* **1991**, *6*, 1578–1583. [[CrossRef](#)]

Disclaimer/Publisher’s Note: The statements, opinions and data contained in all publications are solely those of the individual author(s) and contributor(s) and not of MDPI and/or the editor(s). MDPI and/or the editor(s) disclaim responsibility for any injury to people or property resulting from any ideas, methods, instructions or products referred to in the content.